ULTRASONIC NDE FOR CERAMIC- AND METAL- MATRIX COMPOSITE MATERIAL CHARACTERIZATION

Manohar Bashyam

GE - Aircraft Engines
One Neumann Way, Mail Drop - Q45
Cincinnati, Ohio 45215

INTRODUCTION

A brief summary of the progress of the research in the internal structural characterization of metal matrix (MMC) and ceramic matrix (CMC) composite materials is presented here. These materials show great potential for improving turbine engine performance by enabling operation at higher temperatures and stresses than now possible [1]. However, the application of these materials requires advances in NDE capability in order to characterize material parameters that are likely to affect performance. Several ultrasonic methods are being developed to characterize the internal structure of these anisotropic, inhomogeneous materials.

Our research focuses on characterizing one metal-matrix and two ceramic-matrix composites. The chosen MMC manufactured by Textron, consists of relatively large diameter (140 μm) silicon carbide (SCS6) ceramic fibers in a plasma sprayed titanium 6-4 (Ti64) matrix. Both the CMC materials made by Corning Glass, have a calcium aluminum silicate (CAS) glass-ceramic matrix. One series was reinforced with SCS6 fibers and the other with 15 μm diameter silicon carbide (Nicalon) fibers. The micrographs of these composites are shown in Figs. 1a - 1c to illustrate the relative size of the fibers. Various types of defects were deliberately introduced into these panels by the manufacturer, to simulate delamination, porosity, fiber breakage and matrix cracking etc.

A desirable composite should contain layered, uniformly spaced fibers. Fig. 1 illustrates one potential defect condition of interest, where the fiber distribution is uneven. Note that incomplete bonding or cracking between fibers is also present to some extent. We are also concerned with defects such as fiber breakage, misaligned fibers, incorrect fiber volume fraction, porosity in the matrix and delamination.

This paper discusses ultrasonic velocity, attenuation, backscatter and surface wave techniques to characterize the internal structural features of the MMC and CMC materials.

Review of Progress in Quantitative Nondestructive Evaluation, Vol. 10B
Edited by D.O. Thompson and D.E. Chimenti, Plenum Press, New York, 1991

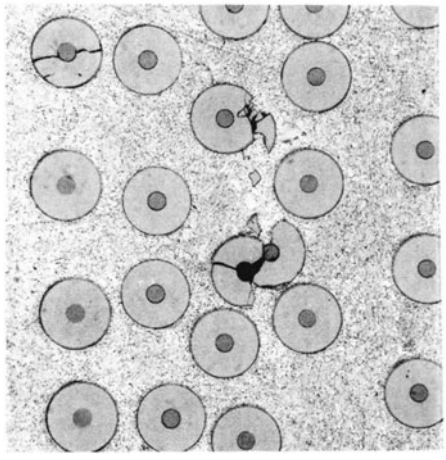

Fig. 1a. Micrograph of a Ti64-SCS6 MMC with 35% fiber volume fraction.

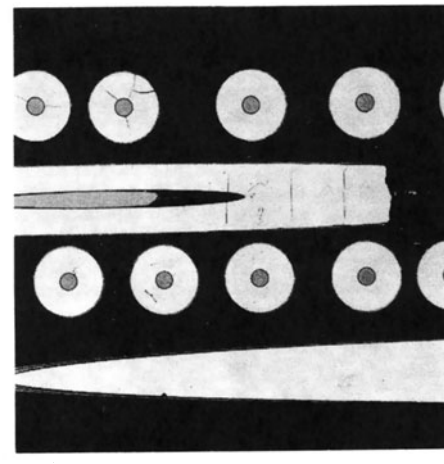

Fig. 1b. Micrograph of a CAS-SCS6 CMC with 45% fiber volume fraction.

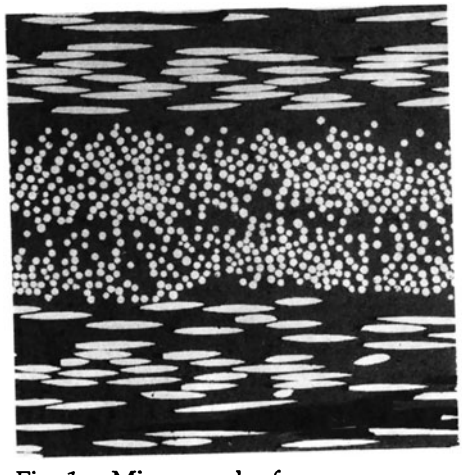

Fig. 1c. Micrograph of a CAS-Nicalon CMC with 45% fiber volume fraction.

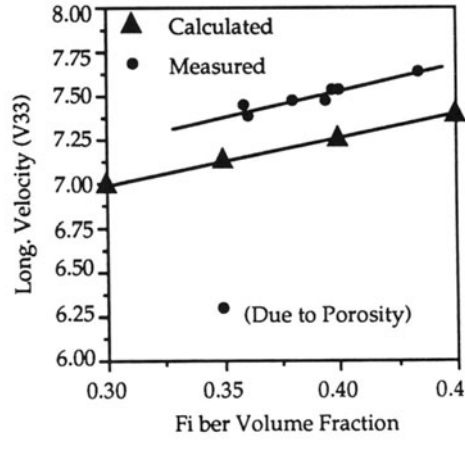

Fig. 2. Theoretical and experimental velocity (V33) for CAS-Nicalon.

VELOCITY MEASUREMENTS

The key to reliable ultrasonic measurements is the thorough understanding of the material properties and the resulting wave propagation modes. For this a previous wave propagation model developed by Murakami & Hegamier [2] was used as the basis of our analyses. This model was used to calculate laminate elastic constants and various ultrasonic wave velocities. Table 1 shows a comparison of the theoretically computed and experimental wave velocities.

The experimental values for the MMC and CMC were lower than the theoretical values predicted by the model with a nominal 35% and 45% fiber

volume fraction respectively. We estimated from the micrographs that the actual volume fractions were lower than the nominal, this resulted in lower experimental wave velocities. This led us to calculate the variation in velocity as a function of fiber volume fraction. Thus varying the fiber volume fraction of the CMC (with Nicalon fibers) between 30% - 45% to compute V_{33} resulted in the graph shown in Fig. 2. The corresponding experimental results are also plotted on the same graph. Note that the fiber volume fractions associated with these results are based on manufacturing estimates. It was seen that a 2% change in volume fraction produced a 1% change in velocity. This clearly indicates a potential NDE method to characterize the fiber volume fraction which is an important variable affecting both the strength and the modules.

To better understand the anisotropic behavior of the composite materials, the Christofel's equation [3] was solved for these materials. The slowness plot (inverse of the velocities) shown in Fig. 3 for two different materials (graphite-epoxy and Ti64-SCS6) for 0° azimuthal angle, i.e. along the fiber direction, illustrates the degree of anisotropy of the materials. The corresponding wave propagation modes for these materials are shown in Fig. 4.
These modes are computed by taking the dot product of the particle velocity and the wave vector, for 0° azimuthal angle, where the value of 1 clearly represents a pure longitudinal mode, value of 0 represents a pure shear mode (PT) and values between 0 and 1 correspond to quasi modes (QL & QT). From these figures it was concluded that the materials are mildly anisotropic when compared to a graphite-epoxy composite material. The slowness and mode plots for CAS-SCS6 and CAS-Nicalon materials were very similar to that of the Ti64-SCS6 plots shown.

ATTENUATION MEASUREMENTS

Previous studies indicate that planar defects such as delaminations should produce attenuation which is relatively independent of frequency. Scatter sources such as porosity produce attenuation which is highly frequency-

Table 1. Comparison of the computed theoretical and experimental wave velocities.

Direction (Km/Sec)	Theoretical	Measured	Theoretical	Measured
	Ti64-SCS6 (35% FF)		CAS-Nicalon (45% FF)	
V_{11}	8.0	~	7.6	~
V_{33}	7.2	7.0	7.4	7.2
V_{44}	3.9	3.9	4.5	4.1
V_{55}	4.1	3.7	4.4	4.1
V_{s1}	3.8	3.6	4.0	3.6
V_{s2}	3.8	3.6	4.0	3.6

~ - Not measured.
V_{11} - Longitudinal along fibers. V_{33} - Longitudinal across fibers.
V_{44} - Shear perpendicular to fiber. V_{55} - Shear along the fiber.
V_{s1} - Surface wave velocity along fiber. V_{s2} - Surface wave velocity across fiber.

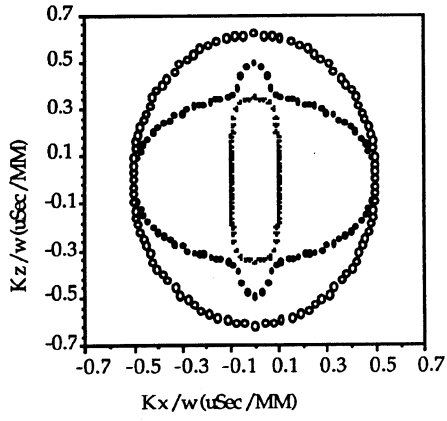

Fig. 3a. Slowness plot for graphite-epoxy - 60% fiber volume fraction at 0° azimuthal angle.

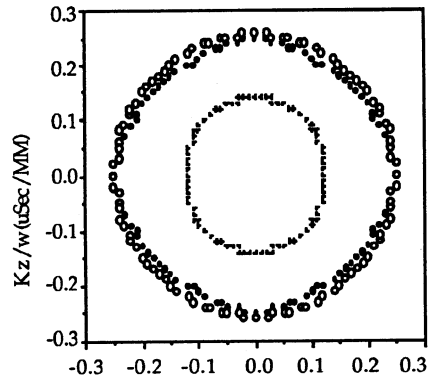

Fig. 3b. Slowness plot for Ti64 -SCS6 - 35% fiber volume fraction at 0° azimuthal angle.

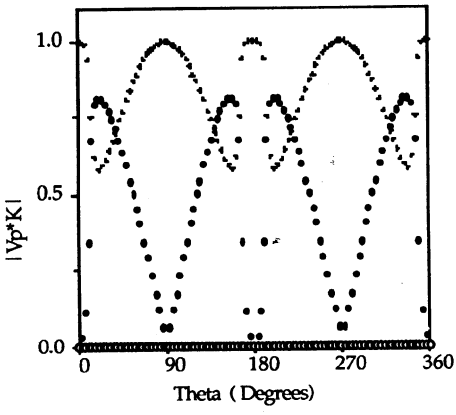

Fig. 4a. Wave propagation mode plot for graphite-epoxy - 60% fiber volume fraction at 0° azimuthal angle.

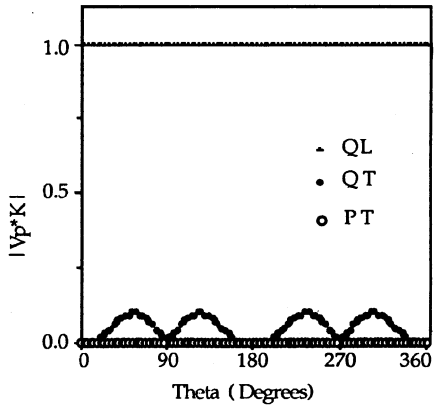

Fig. 4b. Wave propagation mode plot for Ti64-SCS6 - 35% fiber volume fraction at 0° azimuthal angle.

+ - Quasi Longitudinal (QL), * - Quasi Transverse (QT), ° - Pure Transverse (PT)

dependent. Obviously we need to understand the frequency-dependent attenuation characteristics to determine the optimum frequencies for routine inspection.

Two different system configurations were set up for data acquisition, both with broadband transducers. The single-transducer method uses echoes from the front and back surfaces at normal incidence while the through-transmission method uses signals transmitted through the water path as a reference signal. The latter configuration has a wider application since it can be used in attenuative regions where there is no distinct back wall echo.

The reference signal data for a CAS-Nicalon ceramic plate was collected with only water between the transducers. The plate was then inserted and the through-transmitted signal data was collected. The relevant portions of each signal were gated and a FFT was performed to obtain an amplitude versus frequency spectrum for each signal. We then applied a bandpass filter to select the frequency range, typically 2 to 10 MHz. The attenuation versus frequency plot obtained by the division of the two spectra is shown in Fig. 5.

The lower curve shows the averaged attenuation characteristics for non-defective regions obtained from six different CAS-Nicalon plates. This curve was used to compare with the other areas which had programmed defects. Delaminations were produced by replacing a local single layer disc of composite with a layer of dry fibers without the glass-ceramic matrix. Porosity was introduced by varying the conditions of the "burn-out" stage in which organic components are driven from the laminate. It can be seen in Fig. 5 that the attenuation for the non-defective material is very low, with a maximum of 10 dB/cm implying that scattering from the fibers is not predominant. The porosity curve shows the expected increase in attenuation with frequency resulting from scattering from the voids. The curve associated with delamination is not flat, as may be expected from a simple planar defect but is less dependent on frequency than the porosity curve. This may be due to the fact that delamination is not a true planar discontinuity but is a single layer with partial transmission through the fibers and this causes some frequency-dependent characteristics to surface.

OBLIQUE INCIDENCE

In order to solve fiber-related problems such as fiber alignment, ply layup orientation, to improve porosity detection and to detect subsurface cracks, the oblique incidence technique was explored as a viable solution. This technique [4,5,6] has been proven to be very sensitive to fiber orientation and porosity level. The Surface Acoustic Wave (SAW) technique was utilized to find subsurface cracks.

A schematic of the experimental setup for backscatter measurement is shown in Fig. 6. By measuring the backscattered signal, fiber orientation and other fiber related defects can be detected [6].

In Fig. 7, a $[0/90]_{4s}$ CAS-Nicalon panel was scanned to show the four sharp backscattered signals associated with the 0° and 90° fibers. The fibers were initially aligned 45° to the transducer. The specimen was then rotated 360° (shown circumferentially) while the transducer was swept from 10° to 20° (shown radially) past the second critical angle. The layers closer to the front surface showed a higher backscatter amplitude than the ones further down. This proved to be quite useful in identifying the overall layup sequence. This technique could be further improved to show the total number of plies and their orientation. We observed that the material was not sensitive to the incidence angle (α = 10° - 20°). This made the detection of the fiber orientation much easier than expected.

Fig. 8 displays a through-transmission C-scan that was generated using a pair of of 10 MHz (1/2" diameter) broadband transducers. Using the results

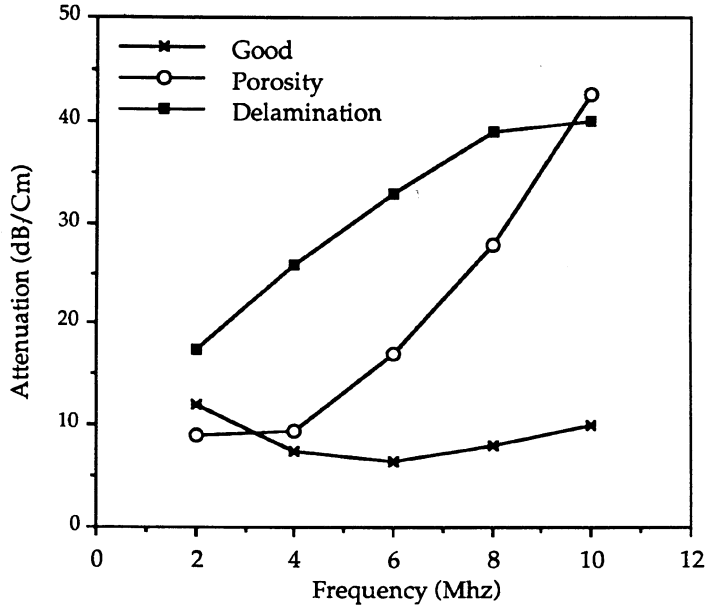

Fig. 5. Attenuation vs frequency plot for CAS-Nicalon CMC material.

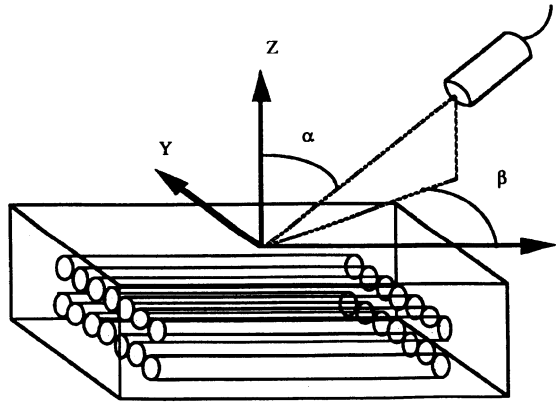

Fig. 6. Experimental setup used for backscatter measurement.

from the scan in Fig. 7, a raster scan of a CMC specimen was performed with a chosen optimum incident angle (α) of 14°, to map the backscattered amplitude (Fig. 9). The comparison of Figs. 8 and 9 indicated that the backscatter method has a higher sensitivity to porosity detection than the through-transmission method.

To detect the subsurface cracks that may be present, we used a low frequency (5 MHz, 1.0" focus) SAW transducer to perform a through-transmission image of the sub-surface. Several researchers have shown the use of the SAW transducer to generate subsurface waves [7]. This approach was taken to image the CMC material with Nicalon fibers. This C-scan (Fig. 9) revealed considerable crack-like indications. On examining the micrographs of

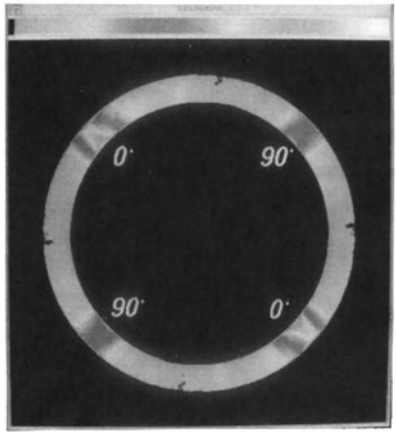

Fig. 7. Polar backscatter scan showing the 0/90° fibers in a [0/90] 4s CAS-Nicalon CMC.

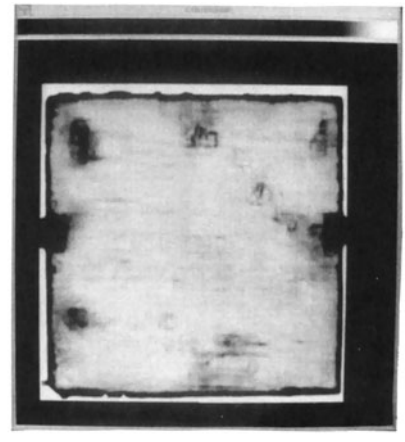

Fig. 8. Through transmission C-scan of a [0/90]4s CAS-Nicalon CMC with moderate porosity.

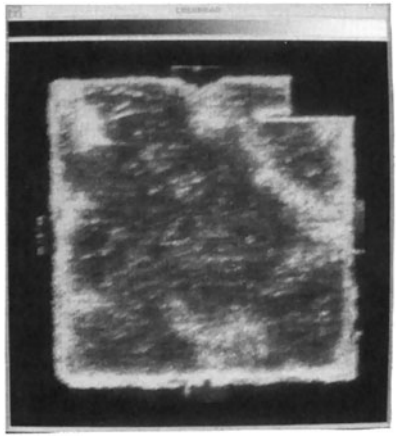

Fig.9. Backscatter scan of a [0/90]4s CAS-Nicalon CMC with moderate porosity.

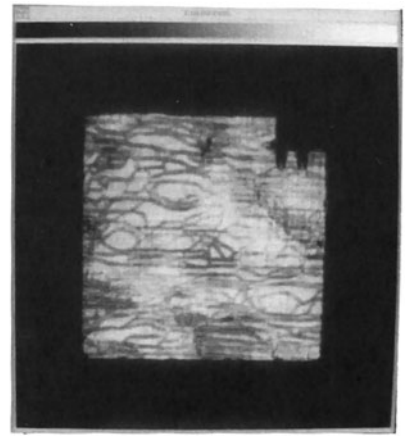

Fig. 10. Surface acoustic wave scan of a [0/90]4s CAS-Nicalon CMC with moderate porosity and subsurface defects.

this material we concluded that these indications were due to the cracks and/or due to the inhomogenieties in the matrix. We expect that the further development of this technique will aid in determining the complete material stiffness matrix.

SUMMARY

We have a theoretical model to calculate elastic properties and ultrasonic velocities for a variety of materials. This model has proven suitable for parametric studies to examine effect of varying fiber volume fractions and porosity among other things.

The materials used in experiments seem to be mildly anisotropic in contrast with graphite-epoxy composites. The low attenuation properties of the MMC and CMC materials make it practical to measure sound velocities. We also noted that the velocity transverse to the fibers is an useful indicator of the fiber volume fraction.

The measurement of frequency-dependent attenuation has proven to be very useful to classify defects. We have a practical method to acquire and process signals and our results indicate that this method has the potential to distinguish between porosity and planar type defects. For large scale operations, it would be necessary to optimize this inspection procedure. One rewarding approach could be the use of real-time DSP filtering techniques to extract two or three frequencies of interest instead of analyzing the entire waveform and spectrum.

We have identified polar backscatter technique to analyze fiber orientation and other fiber related defects. The backscatter technique has contributed to improving the sensitivity of porosity detection for the MMC and CMC materials. We have demonstrated that low frequency SAW has the potential to detect sub-surface defects, porosity and material inhomogeniety.

In our on-going research we have identified several potential techniques that can be implemented from the practical standpoint of NDE of advanced composites. We propose to utilize the frequency dependent backscatter signal in characterizing other difficult to detect fiber related defects. We anticipate that further developments in surface wave technique will aid in determining the complete material stiffness constants.

ACKNOWLEDGEMENT

This work is sponsored by the USAF/WRDC under contract F33615-88-C-5433.

REFERENCES

1. McConnell, V.P., 1990, "Metal Matrix Composites: Materials in Transition - Part I", Advanced Composites, May/June, Vol. 5, No. 3.

2. Murakami, H., and Hegamier, G.A., 1986, "A Mixture Model for Unidirectionally Fiber-Reinforced Composites.", ASME Journal of Applied Mechanics, Vol. 53.

3. Auld, B.A., 1973, "Acoustic Fields and Waves in Solids", Vol. I and Vol. II, (John Wiley & Sons, N.Y.).

4. Rose, J.L., Pilarski, A., and Huang, Y., 1988, "Surface Wave Utility in Composite Material Characterization", Symposium, ASME AMD, Vol. 9D.

5. Rose, J.L., Nayfeh, A., and Pilarski, A., 1989, "Surface Waves for Material Characterization", ASME AMD.

6. Bar-Cohen, Y., and Crane, R.L., 1982, "Acoustic-Backscattering Imaging of Subcritical Flaws in Composites",Materials Evaluation, Vol. 40.

7. Gilmore, R.S., Tam, K.C., Young, J.D., and Howard, D.R., 1986, "Acoustic microscopy from 10 to 100 MHz for industrial applications", Phil. Trans. Royal Society, A320.